

# Reactive power capability analysis of a photovoltaic generator for large scale power plants

*A. Cabrera-Tobar\*, E. Bullich-Massagué\*, M. Aragüés-Peñalba\*, O. Gomis-Bellmunt\**

*\* CITCEA-UPC, Universitat Politècnica de Catalunya, Barcelona, Spain (ana.cabrera@citcea.upc.edu)*

**Keywords:** PQ capability, PV inverter, PV plant.

## Abstract

Currently, the installation of photovoltaic power plants (PVPPs) integrated with the transmission system is becoming common. This interconnection must obey the grid codes of the transmission system operator. The requirements of these grid codes are related to the response during faults, frequency, voltage support, and the regulation of active and reactive power. Because of these requirements, it is necessary to analyse the limitations of the photovoltaic (PV) generators. Accordingly, this paper focuses on the mathematical analysis of the reactive power capability curve of a PV generator considering the variation of solar radiation and temperature. In addition, a PVPP of 1 MW is modelled and simulated in DiGSILENT PowerFactory validating the results.

## 1 Introduction

During the last decade PVPPs have been introduced in the transmission system for utility purpose. Due to this reason new grid codes have been developed to permit that these PVPPs will operate as similar as possible to conventional power plants. The requirements of these grid codes are related to the response during faults, the frequency and voltage support, and the control of the active and reactive power [1]. Because of this new trend of application of the photovoltaic energy, broad studies are necessities in order to understand the challenges that the technology has to face to comply the grid codes. One of these challenges is to understand the PQ capability curves that a PVPP can have considering each of the main components and the different variables that affect its performance as the ambient conditions.

The PQ capability curves for small PV inverters have been studied by a few researchers. For instance, Alonso Albaracín [2] studies the reactive power limits of a small two stage (dc-dc and dc-ac) PV inverter. The analysis is developed for a single PV panel where the dc-dc converter has the duty to step up the voltage and to work at maximum power point. Because it is a small system, the variation of the dc voltage is not considered. It also does not consider the pulse modulation factor. Another example is the research developed by F.Delfino and et al. [3], that obtains the PQ chart for a PV generator (PV panel

and one stage PV inverter). The analysis considers the variation of index modulation, but assumes that the dc voltage is constant. In both studies the implication of solar radiation or temperature have not been considered neither in the control or in the analysis. They also do not consider the variation of the dc voltage to control the power at different points. In the case of Wind power plants, depth studies about the PQ capability curve have been developed considering the limitations of the wind turbine and the converter [4], [5]. Similar studies considering the variation of solar radiation, temperature and dc voltage are necessary in order to have the PQ capability curve for LS-PVPPs application. Accordingly, the present article studies the reactive power capability of a PV generator (PV array and a single stage PV inverter) considering the variation of solar radiation and temperature. The study is developed considering a PV generator of 1 MVA that has two PV inverters and one step up transformer. DiGSILENT PowerFactory is used as a tool to corroborate the mathematical analysis.

The article is structured as follows: Section II explains the topology and the components of the PVPP. In section III, the mathematical model of the different components is explained. In section IV, the analysis of the PQ capability of the PV generator is developed. In section V, a PVPP is simulated in DiGSILENT PowerFactory to understand the relationship between all the variables considered in this study. Finally, conclusions are argued in Section VI.

## 2 PVPP configuration

A PVPP has three basic components: PV panels, inverters and transformers. The connection between the components has different configurations: central, string, multistring and ac-module [6]. These topologies have different robustness, reliability and flexibility. However, the main drawback to overcome in each of them is the response of the maximum power point tracker (MPPT). This control takes the maximum power output of the PV panel at different ambient conditions. If the inverter has several thousands of PV panels, the MPPT is not accurate and it causes mismatches of power. Though this drawback, the most used configuration is the central one because of its robustness and simplicity.

In this article, the configuration used by the PV generator is the central configuration. So, it will have a PV array with thousands of PV panels and one single inverter. The PVPP will

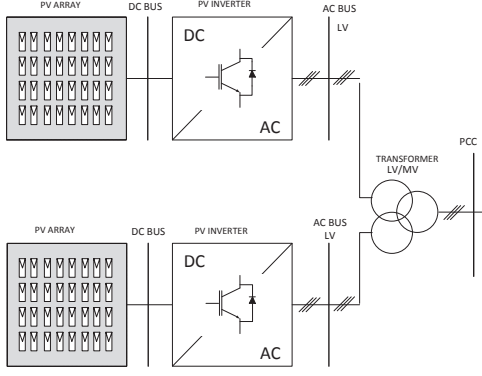


**Figure 1:** Configuration of the PVPP

have two PV generators and one step up transformer of three windings (Figure 1). This structure is commonly used in large-scale PVPPs (e.g. the 9.4 MW PVPP presented in [7]).

### 3 Model of the PVPP

The main component of a PVPP is the PV generator, where the PV array is represented as a source of current, connected in parallel with a capacitor and the inverter will be modelled as a two level voltage source converter (VSC). This section discusses about the model of the PV array and the PV inverter that will be implemented in DiGSILENT PowerFactory.

#### 3.1 PV array model

The behaviour of the PV array depends on the fluctuation of solar radiation during the day [8]. The general model of the PV panel will be developed according to single diode model [9]. In this model, the main variables to consider are: open circuit voltage ( $V_{oc}$ ), short circuit current ( $I_{sc}$ ), solar radiation ( $G$ ), temperature ( $T$ ), correction factor ( $k_v$ ), series and parallel resistances ( $R_s, R_p$ ). The output current ( $i_{pv}$ ) of the PV cell depends on the photogenerated current ( $i_{ph}$ ), the diode current ( $i_d$ ) and the parallel current ( $i_p$ ). The calculation of these values depend on the thermal voltage ( $v_t$ ), the diode voltage ( $v_d$ ) and the voltage at the terminals of the PV panel ( $v_{pv}$ ). The thermal voltage ( $v_t$ ) relates the Boltzmann constant ( $k_B$ ), the number of solar cells interconnected in series in the PV panel ( $N_{ser}$ ), the temperature at standard conditions ( $T_{stc}$ ) and the electron charge ( $q$ ). The following equations are the basic expressions for the calculation of the total current.

$$i = i_{ph} - i_d - i_p \quad (1)$$

$$i_{ph} = i_o \cdot e^{\frac{v_d}{v_t}} + \frac{V_{oc}}{R_p} \quad (2)$$

$$i_d = i_o \cdot e^{\frac{v_d}{v_t}} \quad (3)$$

$$v_t = k_b \cdot N_{ser} \cdot \frac{T_{stc} + 273}{q} \quad (4)$$

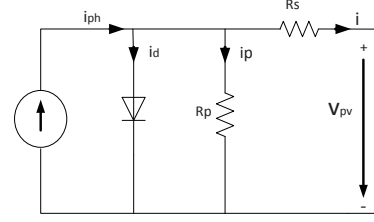


**Figure 2:** Model of the PV cell

At standard conditions, the ( $I_{stc}$ ) and ( $V_{stc}$ ) are obtained considering the equation above. When the ambient temperature ( $T_a$ ) and solar radiation ( $G$ ) change, the solar cell temperature ( $T_c$ ) is affected. This temperature is related to the normal operating cell temperature (NOCT), as it is calculated in the equation (5). With the variation of temperature, the variables that are directly affected are the voltages ( $v_t, V_{oc}$ ) and any other voltage calculated at standard conditions ( $V_n$ ), as equation (6) shows.

$$T_c = T_a + G \cdot \frac{NOCT - 20}{800} \quad (5)$$

$$V_n = V_{stc} + k_v \cdot (T_c - 25) \quad (6)$$

Due to solar radiation, the photogenerated current also changes  $i_{phn}$  as it is shown in equation (7). However, this equation only works if the solar radiation is higher than  $125 \text{ W/m}^2$  [10]. For lower radiations, the expression is as the one indicated in equation (8).

$$i_{phn} = i_{phstc} \cdot \frac{G}{G_{stc}} \quad G > 125 \text{ W/m}^2 \quad (7)$$

$$i_{phn} = i_{phstc} \cdot \frac{0.008 \cdot G^2}{G_{stc}} \quad G < 125 \text{ W/m}^2 \quad (8)$$

Considering these new values, the final equation of the current is:

$$i_n = \frac{i_{phn} - i_{dn} - v_{pv}/R_p}{1 + R_s/R_p} \quad (9)$$

The total current of the PV array ( $I_{array}$ ) is calculated considering the number of strings connected in parallel ( $N_{par}$ ). Meanwhile, the voltage of the PV array ( $V_{array}$ ) is calculated considering the panel voltage ( $v_{pv}$ ) times the number of panels connected in series in each string. These equations are expressed as:

$$I_{array} = i_n \cdot N_{par} \quad (10)$$

$$V_{array} = v_{pv} \cdot N_{ser} \quad (11)$$

#### 3.2 PV inverter model

In the present work one stage of PV inverter is chosen based on VSC converter. In this model a total reactance of the filter and the transformer is considered, meanwhile the total resistance

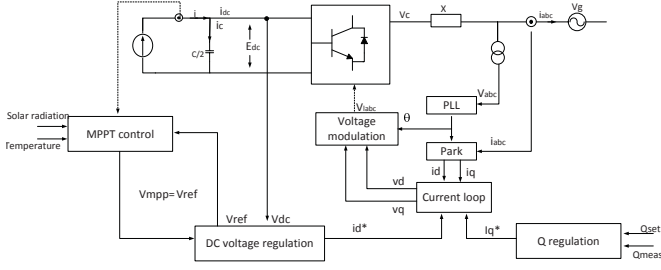


**Figure 3:** Basic PV inverter control

is neglected. The basic control of the PV generator consists of a MPPT control, a dc voltage control, the voltage modulation, the grid synchronization, the current loop control, and the active and reactive power control (Figure 3). In this model as the technology of the PV panels is known, the MPPT calculates the voltage ( $V_{mpp}$ ) at each solar radiation and temperature considering the thermal model of the PV panel explained before. This is the reference voltage that the control of the dc voltage has to follow according to a minimum and a maximum limitation. This limitation is given by the inverter, in which the ac voltage depends on the dc voltage and the modulation technique chosen. In this case as SPWM modulation is chosen, the output line to line voltage  $V_{ac}$  is expressed as the equation (12), where ( $I_m$ ) is the modulation index. This modulation index can vary from 0 to 3.24 [11] depending on the application. In this case, the ( $I_m$ ) will vary from 0 to 1 to work in the linear area. So, the minimum permitted dc voltage is given by the maximum Index modulation ( $I_m = 1$ ). The maximum dc voltage depends on the open circuit voltage of each panel times the number of panels connected in series and the modulation index will vary accordingly (0 to 1). So, the  $V_{mpp}$  can vary between the  $V_{dcmin}$  and the  $V_{dcmax}$  (Figure 4) accepted by the PV inverter. Out of these limits, the inverter will not supply active or reactive power. These limitations are expressed as:

$$V_g = \frac{\sqrt{3}}{2\sqrt{2}} \cdot V_{dc} \cdot I_m \quad (12)$$

$$V_{dcmin} = \frac{2\sqrt{2}}{\sqrt{3}} \cdot V_g \quad (13)$$

$$V_{dcmax} = V_{oc} \cdot N_{ser} \quad (14)$$

The equations of the active power of the PV generator considering solar radiation, temperature, the  $V_{mpp}$  and the efficiency of the inverter (n) are detailed in:

$$P = V_{mpp}(G, T) \cdot I_{dc}(G, T) \cdot n \quad (15)$$

After the mathematical model of the PV array and the inverter, the reactive power capability curve is extracted and explained in the following section.

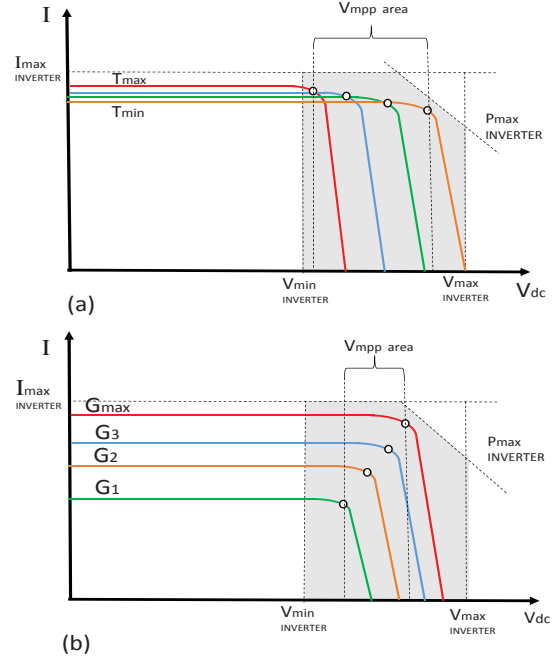


**Figure 4:** Safe operation area of the inverter considering the I-V curve characteristic of the PV array and the inverter (a) Constant solar radiation and variable Temperature, (b) Constant temperature and variable solar radiation

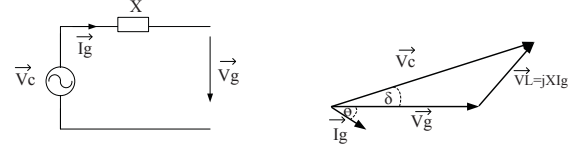


**Figure 5:** Simplified model of the Inverter and its phasor diagram

## 4 PQ capability curve

For this analysis, the simplified model that is considered is illustrated in Figure (5), where the converter is considered as an ideal source of fundamental voltage. The reactor represents the reactance at the point of common coupling (PCC) with the internal grid and the resistance is neglected. Considering this circuit, a basic phasor diagram is in Figure (5). The relation between the active and reactive power with the phase angle ( $\delta$ ), the reactance (X) and the voltages are detailed in equations (16) and (17).

$$P = 3 \cdot \frac{V_g \cdot V_c}{X} \cdot \sin(\delta) \quad (16)$$

$$Q = 3 \cdot \frac{V_g}{X} \cdot (V_c \cdot \cos(\delta) - V_g) \quad (17)$$

The maximum apparent power that the PV generator can inject into the grid is given by the rated power of the converter. Graphically, this limitation is illustrated as a circumference

centered in the origin (Figure 6). The equations for these limitations are (18 and 19). From the P-Q coordinate diagram, the equation (20) is determined. As it was analysed in the dc limitations, the voltage converter depends on the  $I_m$  and the  $V_{dc}$ . So, the new equation is as shown in (21), where the limitations are set by the values of  $I_m$ ,  $V_{dc}$ , grid voltage and the reactance at the PCC.

$$S = 3 \cdot V_g \cdot I_g \quad (18)$$

$$S^2 = P^2 + Q^2 \quad (19)$$

$$P^2 + \left( \frac{3 \cdot V_g}{X} \right)^2 = \left( \frac{V_g \cdot V_c}{X} \right)^2 \quad (20)$$

$$P^2 + \left( \frac{3V_g}{X} \right)^2 = \left( \frac{\frac{\sqrt{3}}{2\sqrt{2}} \cdot V_g \cdot V_{dc} \cdot I_m}{X} \right)^2 \quad (21)$$

The new curve is a circle that has a centre in  $-3V_g^2/X$  in the Q axis with a radius of  $3 \cdot V_g \cdot V_c/X$ . This radio changes according to  $I_m$  and the dc voltage that permits the control of the reactive power similar to the field excitation in a synchronous generator. Also the reactance at the PCC influence in the final value for this radius. In this case, the dc voltage is equal to the  $V_{mpp}$  that is calculated for each solar radiation and temperature. Considering the variable value of  $V_{mpp}$ , the new curve is:

$$P^2 + \left( \frac{3V_g}{X} \right)^2 = \left( \frac{\frac{\sqrt{3}}{2\sqrt{2}} \cdot V_g \cdot V_{mpp}(G, T) \cdot I_m}{X} \right)^2 \quad (22)$$

Besides, these two limitations circles, it is necessary to consider the limitations given by the PV array due to the solar radiation and temperature. The equation (15) relates the active power with the  $V_{mpp}$  and the  $I_{dc}$ , where the  $V_{mpp}$  depends on the cell temperature and the  $I_{dc}$  depends on the solar radiation. With higher solar radiation, the active power increases as the  $I_{dc}$  is higher, but if the temperature is higher than the one calculated at standard conditions, the  $V_{mpp}$  is higher that causes a drastic reduction of current and therefore the active power is reduced. The active power is limited due to meteorological conditions. In the case that the Temperature is constant, the active power is limited by the solar radiation value. The maximum possible power that the PV generator can supply at a given temperature is when the solar radiation is the maximum possible at the location of the PVPP. In the other hand, if the solar radiation is considered constant, the maximum active power that the PV generator can supply is at minimum temperature. Another limitation, is the minimum active power that the PV generator can supply when temperature is high. After this limitation, the voltage  $V_{mpp}$  is lower than the  $V_{dcmin}$ , and thus the system is not working in the area illustrated in Figure 4. With the limitation of the dc voltage, the maximum ambient temperature accepted for the maximum solar radiation at the location is in equation 23. The different limitations discussed above are illustrated in Figure 6.

$$T_{max} = \frac{\frac{2\sqrt{2}}{\sqrt{3}} \cdot V_g - V_{mppstc} \cdot N_{ser}}{k_v \cdot N_{ser}} - G_{max} \cdot \frac{NOCT - 20}{800} + 25 \quad (23)$$

After this mathematical analysis, the next section will show the dependence between the different variables and the PQ capabilities of the PV generator considering the variation of solar radiation, temperature, Modulation Index and the dc voltage by using a simulation software.

## 5 Simulation and Results

In this section the PQ capability curve of a PVPP is extracted considering the equations analysed in the previous section. For this purpose a PVPP of 1 MW is modelled and simulated in DiGSILENT PowerFactory. The PVPP has two PV generators of 0.5 MW each. The main characteristics of the PV generator are detailed in Table 1.

PV panel characteristics		PV array characteristics	
Voc	58.8 [V]	Parray	0.5 [MW]
Isc	5.01[A]	Nser	15
Impp	4.68[A]	Npar	175
Vmpp	47 [V]	Tmin, Tmax	0-70 [C]
kv	0.45[1/°C]	Gmax	1100 [W/m²]

**Table 1:** PV panel and array characteristics

The PVPP will work in underexcited or overexcited operation. To test the PVPP under different solar radiation and temperature, three scenarios are analysed.

- Scenario 1: The solar radiation will vary from 0 to 1000 W/m² with steps of 1 W/m². The ambient temperature is constant  $T = 10^\circ\text{C}$ .
- Scenario 2: The temperature will vary from 10 to 40 °C with steps of 0.1 °C. The solar radiation has a unique value of 1000 W/m².
- Scenario 3: The solar radiation will vary from 0 to 1000 W/m² with steps of 1 W/m². The ambient temperature is constant  $T = 40^\circ\text{C}$ .

The PQ curve of the PVPP at the PCC, for each scenario, is illustrated in Figure 7. In each case, the  $V_{mpp}$  is calculated for every solar radiation and temperature. The variation of  $V_{mpp}$  permits to change the point of operation of the PV generator.

In the first scenario, the active power varies from 0 p.u to 0.99 p.u. that corresponds to the increment of solar radiation when the ambient temperature is 10°C. In underexcited mode, the reactive power limitation corresponds to the circle calculated in equation (19). The absolute value varies from 0.15 p.u to 1 p.u, in which the lower value corresponds to 1000 W/m² and the highest value to 0 W/m². In overexcited mode, the internal limitation corresponds to the variation of  $V_{mpp}$  and  $I_m$  that is almost constant to maintain the balance. In this case this limitation is close to 0.54 p.u. When the solar radiation is higher than 800 W/m², then the limitation corresponds to the equation (19). In the second scenario, the solar radiation



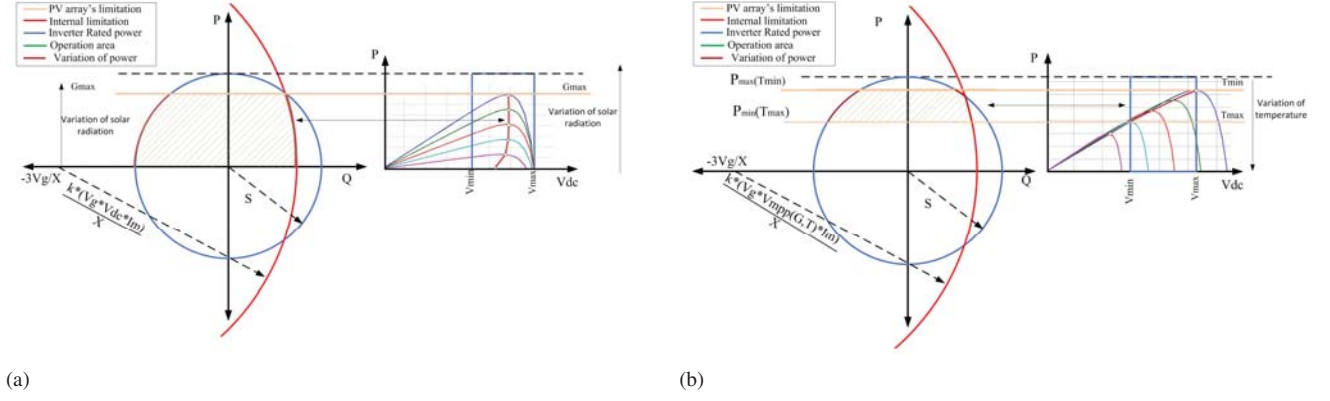


**Figure 6:** PQ capability analysis of the PV generator considering (a) Constant Temperature and variable solar radiation (b) Constant Solar radiation and variable Temperature

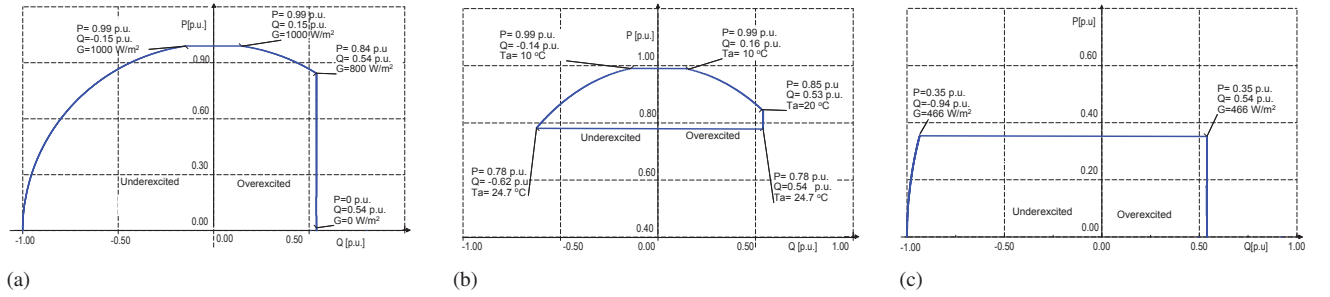


**Figure 7:** PQ capability analysis of the PV generator (a) Scenario 1 (b) Scenario 2 (c) Scenario 3.

is  $1000 \text{ W/m}^2$  and has a variable temperature from  $10^\circ\text{C}$  to  $40^\circ\text{C}$ . The active power varies from  $0.99 \text{ p.u.}$  to  $0.78 \text{ p.u.}$  when the temperature increases. In this case, the maximum temperature permitted by the PV generator is  $24.7^\circ\text{C}$ . In underexcited mode, the absolute reactive power varies from until  $0.62 \text{ p.u.}$ . Lower reactive power corresponds to the temperature of  $10^\circ\text{C}$  and the higher reactive power corresponds to the maximum permitted by the PV generator. In overexcited operation, the reactive power has two limitations. The first one corresponds to the internal limitation that is almost constant with a value of  $0.54 \text{ p.u.}$ . This value is constant when the temperature is between  $20^\circ\text{C}$  to  $24.7^\circ\text{C}$ . Before  $20^\circ\text{C}$ , the reactive power varies from  $0.53 \text{ p.u.}$  to  $0.14 \text{ p.u.}$ . In the third scenario, as the ambient temperature is  $40^\circ\text{C}$ , the maximum solar radiation permitted by the PV generator is  $466 \text{ W/m}^2$ . For higher solar radiations, the active power is 0. The active power varies from 0 to  $0.35 \text{ p.u.}$  when the solar radiation goes from 0 to  $466 \text{ W/m}^2$ . In underexcited mode, the absolute reactive power varies from  $0.94 \text{ p.u.}$  to  $1 \text{ p.u.}$ . In overexcited mode, the internal limitation is almost constant in the range of 0 to  $466 \text{ W/m}^2$  having a value of  $0.54 \text{ p.u.}$ . To understand the variation of reactive power due to the variation of ambient conditions a 3D graph is plotted in Figure 8 for overexcited and underexcited operation. For each temperature a maximum solar radiation is permitted and thus a maximum active and a minimum reactive power can be supplied by the PV generator. In the case that the temperature is

$40^\circ\text{C}$ , the maximum solar radiation permitted is close to  $500 \text{ W/m}^2$ . If the temperature is  $30^\circ\text{C}$ , the maximum solar radiation is close to  $700 \text{ W/m}^2$ . For temperatures of  $20^\circ\text{C}$ , the maximum solar radiation permitted is  $800 \text{ W/m}^2$ . For lower temperature, higher solar radiation can be handled.

## 6 Conclusions

This paper introduced the modelling and the control of a PVPP to evaluate its limitations when it is connected with the grid. It also presents the mathematical analysis of the limitations of the PV generator considering the variation of solar radiation and temperature and using the voltage equal to  $V_{\text{mpp}}$ . Then, a PVPP was simulated in DiGSILENT Power Factory, to understand the effects of each variable on the PV generator. From the mathematical analysis and the simulation some conclusions are discussed.

The variation of active power depends on the solar radiation and the temperature. Maximum active power corresponds to a maximum solar radiation and a minimum temperature. Minimum active power corresponds to the minimum solar radiation permitted by the PV generator to work in a safe area and the maximum temperature of the location. It is also necessary to consider the maximum power that the PV generator can deliver when there are higher temperatures. This temperature limits

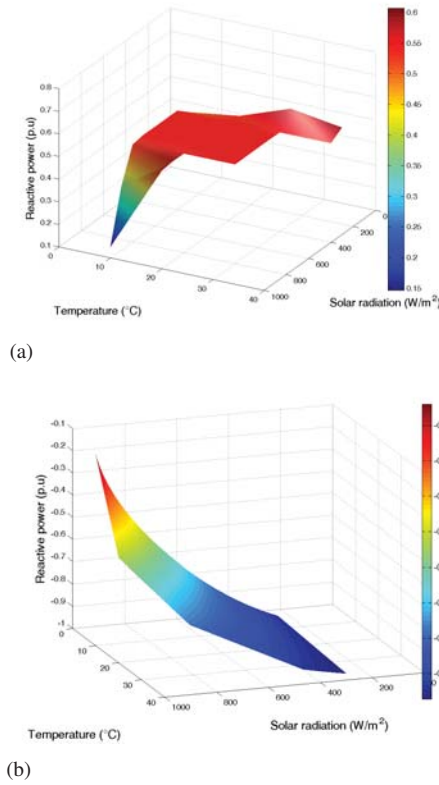


**Figure 8:** Reactive power vs Solar radiation and temperature.  
(a) Overexcited mode (b) Underexcited mode.

the power extracted by the PV generator despite the solar radiation value.

The variation of reactive power depends on the solar radiation and the temperature. Maximum reactive power corresponds to a minimum solar radiation and higher temperature. Minimum reactive power is related to a maximum solar radiation and the minimum temperature. In overexcited mode, the limitation corresponds to the performance of the inverter. It depends on the modulation index, the  $V_{mpp}$  and the  $V_{ac}$ . As the relation of  $V_{mpp}$  with  $I_m$  should be constant, the reactive power also stays constant despite the ambient temperature changes. This value is constant when the solar radiation varies from 0 to  $800 \text{ W/m}^2$  and the temperature is inside  $20^\circ\text{C}$  to  $24.7^\circ\text{C}$ .

The consideration of the voltage equal to  $V_{mpp}$  makes that the PQ capability curve depends on the solar radiation and temperature. The minimum and maximum active and reactive power depends on the location and the ambient conditions. This behaviour is not suitable for LS-PVPPs as they have to comply grid code requirements and to maintain active power constant despite the variation of the ambient conditions. For future work, the variation of voltage will be analysed to see the effect of it on the PQ capability curve.

## Acknowledgements

This work is supported by the National department of Higher Education, Science, Technology and Innovation of Ecuador (SENESCYT).

## References

- [1] BDEW. "Technical Guideline Generating Plants Connected to the Medium-Voltage Network", , (2008), [Online]. Available: <https://www.bdew.de>.
- [2] R. Albarracin, M. Alonso. "Photovoltaic reactive power limits", *2013 12th Int. Conf. Environ. Electr. Eng.*, pp. 13–18, (IEEE, 2013).
- [3] F. Delfino, G. Denegri, M. Invernizzi, R. Procopio, G. Ronda. "A P-Q capability chart approach to characterize grid connected PV-units", , (2009).
- [4] T. Lund, P. Sørensen, J. Eek. "Reactive power capability of a wind turbine with doubly fed induction generator", *Wind Energy*, **10**(4), pp. 379–394, (jul 2007).
- [5] O. Gomis-Bellmunt, F. Hassan, C. Barker, A. Egea-Alvarez. "Capability curves of a VSC-HVDC connected to a weak AC grid considering stability and power limits", *11th IET Int. Conf. AC DC Power Transm.*, pp. 053 (5 .)–053 (5 .), (Institution of Engineering and Technology, 2015).
- [6] A. Cabrera-Tobar, E. Bullich-Massagué, M. Aragüés-Peñalba, O. Gomis-Bellmunt. "Topologies for large scale photovoltaic power plants", *Renew. Sustain. Energy Rev.*, **59**, pp. 309–319, (jun 2016).
- [7] E. Bullich, M. Aragüés, L. Serrano, P. Carlos, R. Ferrer, O. Gomis. "Power plant control in large scale photovoltaic power plants: design, implementation and validation in a 9.4 MW photovoltaic plant.", *IET Renewable Power Generation.*, (2015).
- [8] A. K. Cabrera, H. U. Banna, C. Koch-Ciobotarus, S. Ghosh. "Optimization of an air conditioning unit according to renewable energy availability and user's comfort", *IEEE PES Innov. Smart Grid Technol. Eur.*, pp. 1–7, (IEEE, 2014).
- [9] T. Markvart. *Practical Handbook of Photovoltaics*, (Elsevier, 2012).
- [10] B. Marion. "Comparison of predictive models for photovoltaic module performance", *2008 33rd IEEE Photovoltaic Spec. Conf.*, pp. 1–6, (IEEE, 2008).
- [11] G. Camacho, D. López, J. Díaz, C. Gaviria. "Characterization of the Pulse-Width Modulation (PWM) Techniques Applied to Three-Phase Inverters", *Épsilon*, (2012).